Supplemental Information

Slippery liquid-like surfaces as a promising solution for sustainable drag reduction

Lingxuan Hao, Bei Fan

Department of Mechanical Engineering, Michigan State University, East Lansing, MI, 48823, USA.

The PDF file includes:

Section S1. Scanning Electron Microscopy (SEM) images of surface morphology

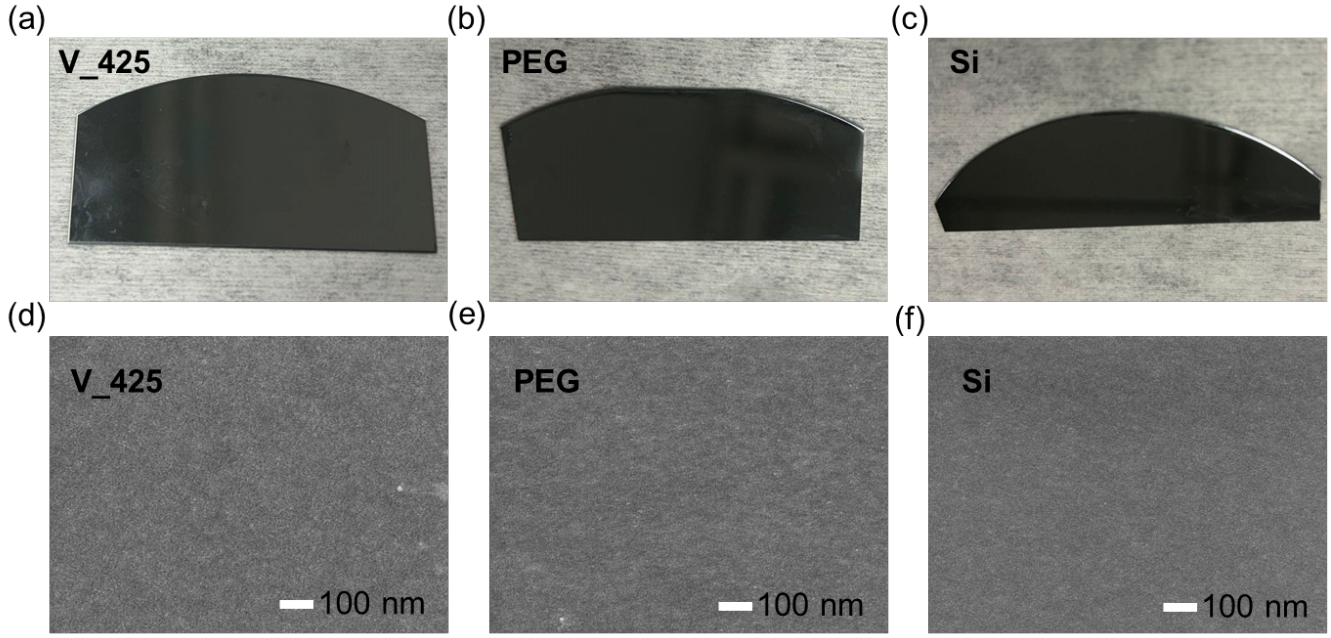

Figure S1. (a)-(c) Pictures of both hydrophobic/hydrophilic slippery liquid-like surfaces and bare Si surfaces. The polymer brush layer on slippery liquid-like surfaces appears as a transparent coating layer with nanometer-thin thickness, making it nearly indistinguishable from the bare Si surface. No visible morphological difference is observed between the slippery liquid-like surfaces with bare Si surface; (d)-(f) SEM images of both hydrophobic/hydrophilic slippery liquid-like surfaces and bare Si surfaces. The SEM images are captured using 7500F SEM at 100,000 times magnification. The SEM analysis reveals the smooth and uniform surface morphology of the polymer brush layer on slippery liquid-like surfaces, further confirming their ultra-smooth, low-inhomogeneity properties.

Section S2. Surface wetting characterization

Table S1.1. Contact angle characterization

	V_425 θ_{left}	V_425 θ_{right}	PEG θ_{left}	PEG θ_{right}
Position1, reading 1	104.3°	104.8°	44.5°	46.4°
Position1, reading 2	104.3°	104.9°	44.5°	46.4°
Position1, reading 3	104.4°	104.8°	44.4°	46.4°
Position1, reading 4	104.4°	104.8°	44.4°	46.3°
Position1, reading 5	104.4°	104.8°	44.4°	46.3°
Position1, reading 6	104.5°	104.8°	44.5°	46.2°
Position1, reading 7	104.3°	104.8°	44.4°	46.3°
Position1, reading 8	104.3°	104.7°	44.5°	46.2°
Position1, reading 9	104.3°	104.8°	44.4°	46.2°
Position1, reading 10	104.2°	105.8°	44.4°	46.2°
Position2, reading 1	104.1°	104.6°	41.3°	41.7°
Position2, reading 2	104.0°	104.6°	41.3°	41.6°
Position2, reading 3	104.0°	104.6°	41.2°	41.6°
Position2, reading 4	104.0°	104.6°	41.2°	41.6°
Position2, reading 5	104.0°	104.6°	41.2°	41.6°
Position2, reading 6	104.0°	104.6°	41.2°	41.6°
Position2, reading 7	104.0°	104.6°	41.1°	41.6°
Position2, reading 8	104.1°	104.4°	41.2°	41.5°
Position2, reading 9	104.1°	104.5°	41.0°	41.7°
Position2, reading 10	104.0°	105.5°	41.2°	41.4°
Position3, reading 1	105.4°	104.8°	39.7°	39.7°
Position3, reading 2	105.4°	104.9°	39.7°	39.8°
Position3, reading 3	105.4°	104.8°	39.9°	39.5°

Position3, reading 4	105.4°	104.8°	39.6°	39.7°
Position3, reading 5	105.4°	104.8°	39.7°	39.6°
Position3, reading 6	105.3°	104.8°	39.6°	39.7°
Position3, reading 7	105.3°	104.8°	39.6°	39.6°
Position3, reading 8	105.4°	104.7°	39.8°	39.5°
Position3, reading 9	105.3°	104.8°	39.8°	39.4°
Position3, reading 10	105.4°	105.8°	39.5°	39.6°

Table S1.2 CAH characterization

	V_425 θ_{adv}	V_425 θ_{rec}	PEG θ_{adv}	PEG θ_{rec}
Position 1	105.11°	103.41°	45.16°	43.35°
Position 2	105.96°	104.37°	44.96°	43.39°
Position 3	105.67°	104.21°	41.14°	39.32°

Section S3. Microfluidic device assembling

The customized microfluidic device was assembled with a polycarbonate (PC) block as the base of the device, containing the inlet reservoir, outlet reservoir and a rectangular vacancy holding the testing slippery liquid-like surface (SLLS). A thin silicone rubber sheet (0.005") is cut in the center with the aa rectangular shape to determine the microchannel dimensions. Another PC board with pressure sensor port sits on the top of the silicone rubber plays the role as the top wall of the microchannel. The assembling details were illustrated in figure S2.

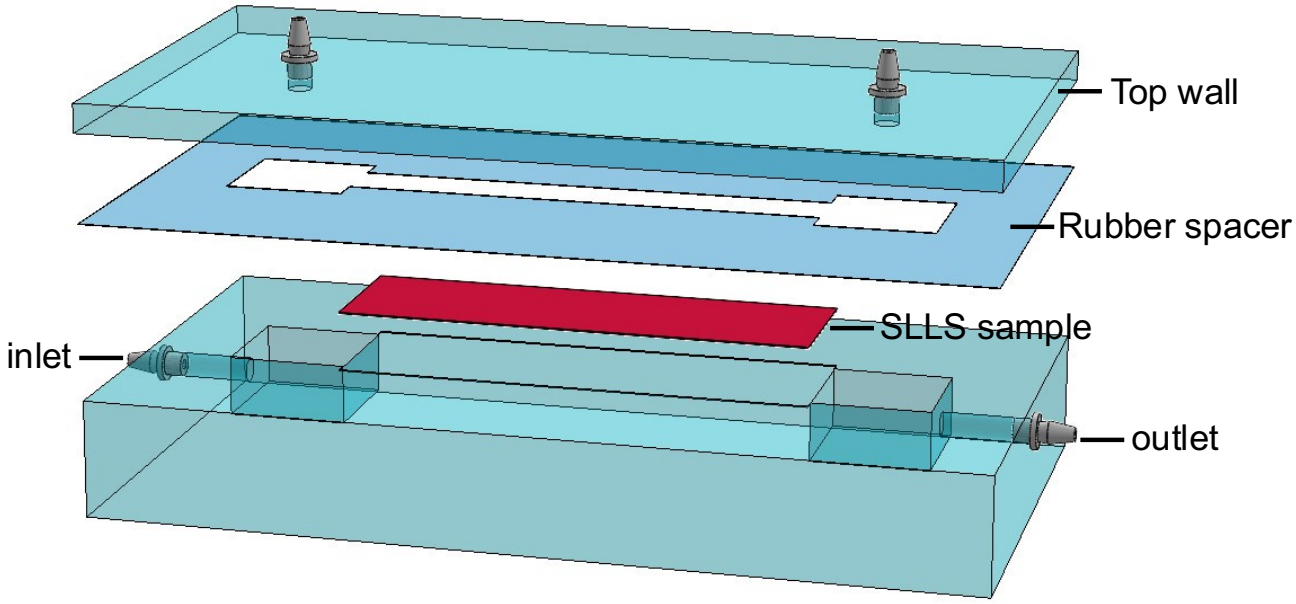

Figure S2. The detailed schematic of microfluidic device assembling. The microchannel is constructed with SLLS as the bottom wall, PC plate as the top wall, and the rubber spacer as the side walls.

Section S4. Pressure drop acquisition with differential pressure sensor

The pressure value across the microchannel was measured with the differential pressure sensor and the results were acquired as voltage signals. The pressure response was measured while the fluid flow was turned on and off to generate the square wave voltage signals. The peak-to-peak voltages were converted to pressure result with linear relationship of 497.08 Pa per volt, calibrated by Omega Engineering. The measurement was repeated five times, with each repetition consisting of three cycles. The final result was calculated by averaging all 15 values obtained from the five repetitions. As shown in figure S3, the three cycles of voltage measurements from a single repetition were shown.

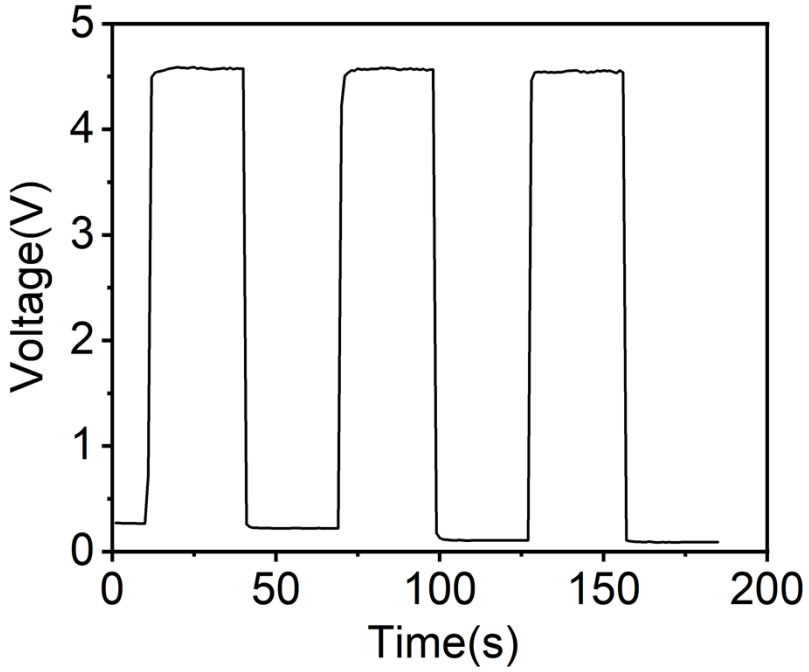

Figure S3. Data acquisition of the differential pressure sensor with voltage signals.

Section S5. Drag reduction validation on bare Si surface

To validate the accuracy of the drag reduction measurement set up, we measured the pressure drop across the bare Si surface and compared the result with theoretical no-slip pressure values. As presented in figure S4, the experimental results fit well with the theoretical no-slip pressure.

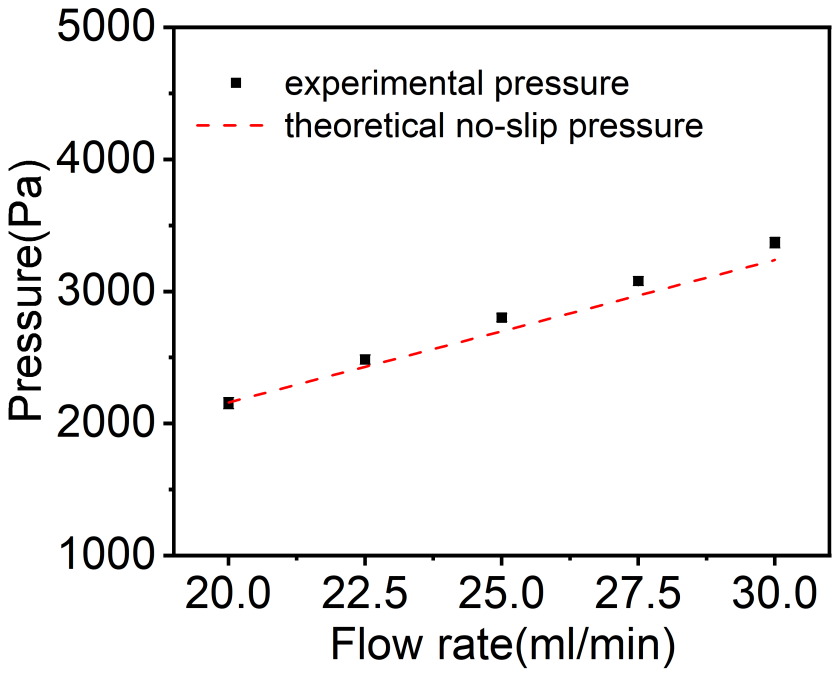

Figure S4. Comparison between the experimental measurement of pressure drop with theoretical no-slip pressure results.

Section S6. Channel height measurement with digital microscopy

The channel height has significant influence on the drag reduction performance. Therefore, the channel height was specifically measured after each experiment. An exact silicone replica of each microchannel was molded before the device was dissembled. The replica was cured at room temperature for 12 hours. The replica was placed on clean Si and the height of each replica was scanned on 3 different locations using a digital microscopy. The replicas were scanned under 200x objective.

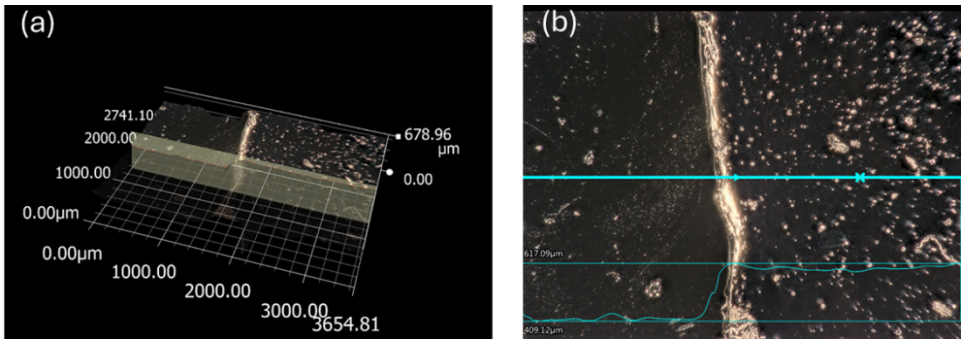

Figure S5. (a) 3-D scanning the edge of replica set on clean Si surface with digital microscopy. (b) The enlarged top view of the scanning region. The white line represents the selected measuring section.

Section S7. Hydrostatic durability of surfaces under different pH level

To assess the acidic and alkaline resistance of SLLS, both V_425 surface and PEG surfaces were immersed in solutions with different pH levels (pH = 1, 4, 10, 13), respectively. The wetting properties (i.e. CA, CAH and SA values) were characterized at 3 different positions every 12 hours until the surface failed. Both slippery liquid-like surfaces failed within couple hours in strong acid (pH = 1) and base (pH = 13) solutions. However, they can maintain the surface properties for over hundreds of hours in relatively weak acid (pH = 4) and base (pH = 10) solutions. In general, the PEG surface demonstrates higher resistance in acidic environment, while the V_425 surface exhibits higher resistance in base environment. The change of CA, CAH and SA values with time of slippery liquid-like surfaces while immersed in weak acid/base solution are shown in figure S6.1. And the lifetime of each slippery liquid-like surface at different pH level is shown in figure S6.2.

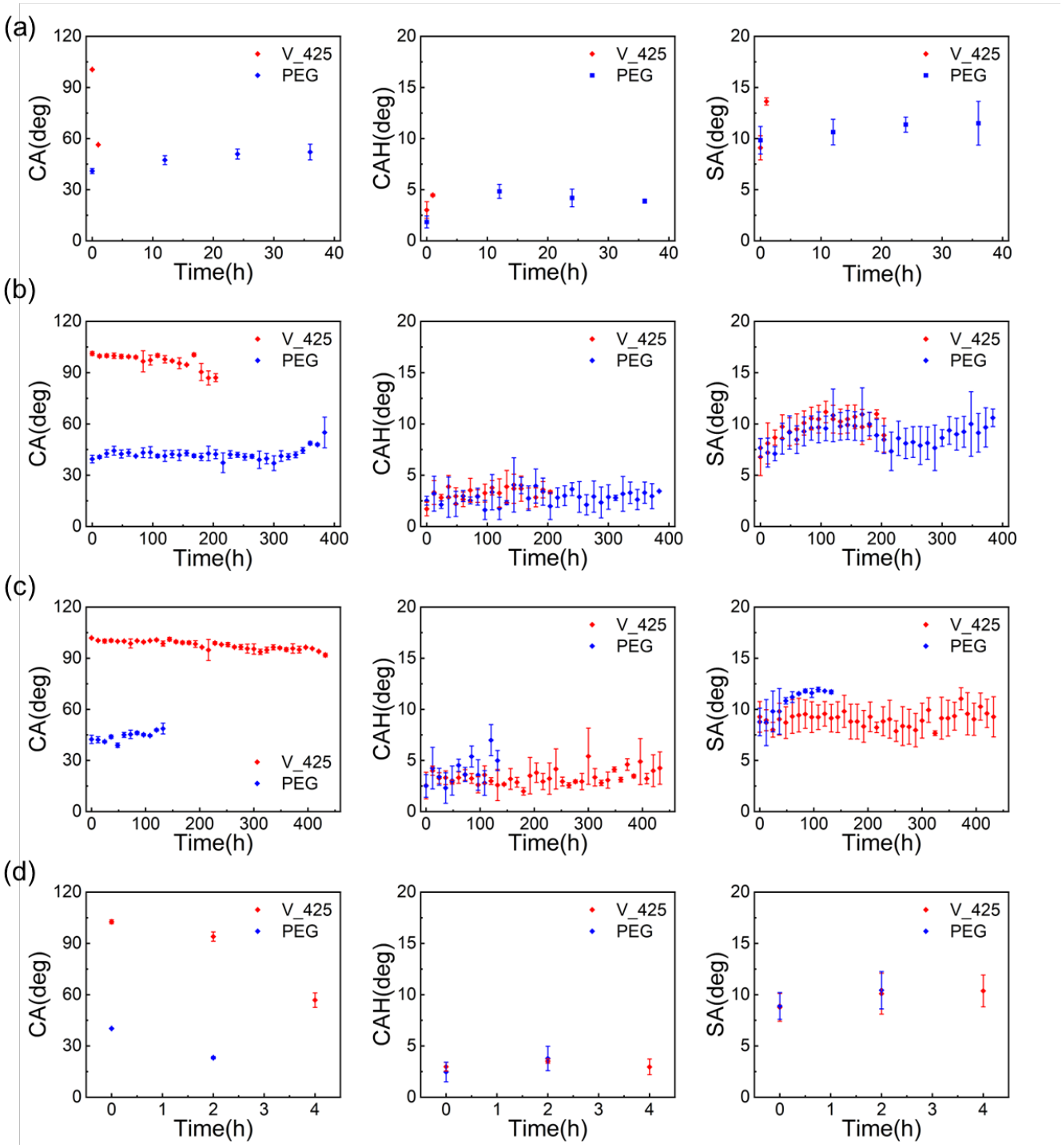

Figure S6.1 (a) Change of wetting properties i.e., CA, CAH, SA, with time of slippery liquid-like surfaces while immersed in pH = 1 solution; (b) Change of wetting properties i.e., CA, CAH, SA, with time of slippery liquid-like surfaces while immersed in pH = 4 solution; (c) Change of wetting properties i.e., CA, CAH, SA, with time of slippery liquid-like surfaces while immersed in pH = 10 solution; (d) Change of wetting properties i.e., CA, CAH, SA, with time of slippery liquid-like surfaces while immersed in pH = 13 solution.

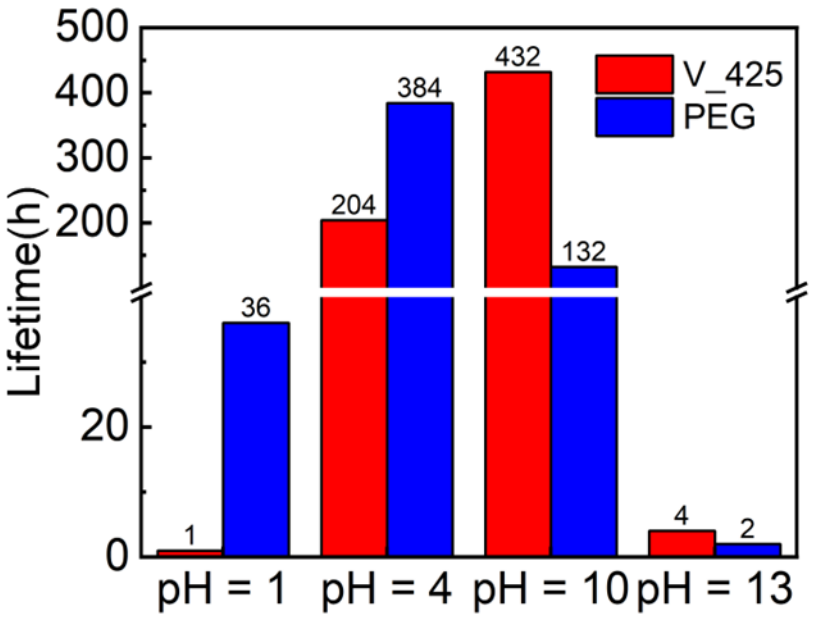

Figure S6.2 Summarization of lifetime of both slippery liquid-like surfaces while immersed in solution with different pH levels